Eur. Phys. J. Special Topics **224**, 3295–3309 (2015)

DOI: 10.1140/epjst/e2015-50084-6

THE EUROPEAN PHYSICAL JOURNAL SPECIAL TOPICS

Review

Dynamics of aerial target pursuit

S. Pal[a]

Mechanical & Aerospace Engineering, University of Central Florida, Orlando, FL 32816, USA

Received 14 April 2015 / Received in final form 2 November 2015
Published online 15 December 2015

Abstract. During pursuit and predation, aerial species engage in multi-tasking behavior that involve simultaneous target detection, tracking, decision-making, approach and capture. The mobility of the pursuer and the target in a three dimensional environment during predation makes the capture task highly complex. Many researchers have studied and analyzed prey capture dynamics in different aerial species such as insects and bats. This article focuses on reviewing the capture strategies adopted by these species while relying on different sensory variables (vision and acoustics) for navigation. In conclusion, the neural basis of these capture strategies and some applications of these strategies in bio-inspired navigation and control of engineered systems are discussed.

1 Introduction

Aerial animals such as insects and bats engage in predation on a daily basis for survival. During predator-target interactions, the complex maneuvers performed by both participants make such behavior particularly challenging. For predators, the task is crucial as their survival depends on the rate of successful target capture. Apart from multi-tasking, predators face uncertainties such as dynamic target trajectory, foraging in complex and unknown environments, and combating prey evasive tactics. Despite such challenges, many of them demonstrate very precise prey capture behavior. As an example, the prey capture success rate in dragonfly has been shown to be in between 76% and 97% by Olberg and coworkers [1].

The success of aerial predation largely depends on efficient navigation of the predator to the target. Hence, the acuity of the predator's navigation system which is strongly tied to it's sensory mode of perception plays a significant role in the pursuit and capture dynamics. In aerial insects, navigation is dependent on vision. Insect vision occurs through "compound eyes" that are made up of repetitive elements or facets called "ommatidia" [2]. As examples, the dragonfly has the largest compound eye among insects and carries as many as 30,000 ommatidia, whereas smaller insects such as the fruit fly or *Drosophila* carry only 1400 ommatidia [3]. Although a multi-faceted eye provides a nice peripheral vision in insects, the quality of such vision is restricted by the immobility, fixed-focus optics and close positioning of the insect compound eyes which limit the range estimation capability and spatial resolution of insects [4].

[a] e-mail: spal@ucf.edu

Contrary to insects, majority of bats (of the order Microchiroptera) rely on the reflections of their emitted acoustic signals (in the range of 20 kHz to 150 kHz) for navigation [5]. The emitted acoustic signals vary in duration and sound pressure level and efficient navigation is dependent on the bat's analysis of spectro-temporal properties such as time delay, intensity, spectrum, interaural time and intensity differences of their echoes [6]. Since most echolocating bats are nocturnal and often forage in cluttered environments, they encounter the daunting task of organizing acoustic information from multiple echoes of their vocalizations based on limited acoustic parameters. Integrating acoustic information with flight dynamics while navigating to targets is another challenging task for these species.

Literature reveals that aerial predators indeed have evolved with navigation strategies for successful capture of their quarry inspite of limitations in their sensory system. This article brings forward to the readers a brief review of the different aerial capture strategies in aerial insects and echolocating bats. The focus is on the dynamics of the simple maneuvers employed by these species in prey capture scenarios and on possible neural linkages in such specific capture maneuvers. In conclusion, how the knowledge gained is providing new insights in the design of biologically-inspired engineered systems are briefly discussed.

2 Pursuit strategies

Most researchers to date have studied prey capture dynamics in aerial insects such as housefly, hoverfly, fruit fly, dolichopodid fly, blowfly, dragonfly and honey bee and in aerial mammals such as echolocating bats. The earliest experimental studies on pursuit behavior were performed on houseflies and hoverflies by Land and Collet. This was followed by subsequent studies on other insects by several other researchers and most recently on echolocating bats. From these experimental studies, the prey capture behavior in aerial insects and echolocating bats can be generalized into five broad categories which will be elaborated in the following subsections.

2.1 Smooth tracking

Smooth tracking is a pursuit mechanism where the pursuer aims at the image of its target straight ahead and strives to minimize the deviation of the target image from straight ahead throughout the pursuit using visual cues. Consequently, the resulting flight path of the pursuer is spiral when the target is located frontally and it moves in the horizontal direction. Target capture is guaranteed only if the pursuer moves faster than the target. Smooth tracking was first detected as a predation mechanism in small houseflies [7]. Subsequent reasearch showed that blow flies, dolichopodid flies and honey bees adopted similar mechanisms in their prey pursuits [8–10].

Collet and Land observed the smooth tracking behavior in an experimental study with small housefly *Fannia canicularis* chasing its conspecifics [7]. The authors proposed that smooth tracking in small housefly was achieved through a simple proportional – derivative (PD) feedback control mechanism. In their proposed model, the angular velocity of the pursuer fly ω_p or the system output was controlled by the input variable, error angle, θ_e. The angle θ_e as illustrated in Fig. 1A refers to the position error of the target relative to the pursuer and is the angle between the pursuer's long axis and the position vector directed from the pursuer to the prey. The angle θ_a in Fig. 1A denotes the absolute angle which is the direction angle of the the position vector with respect to the positive x-axis. The angle θ_P in Fig. 1A denotes the angular position of the pursuer with respect to positive x-axis. Figure 1B shows

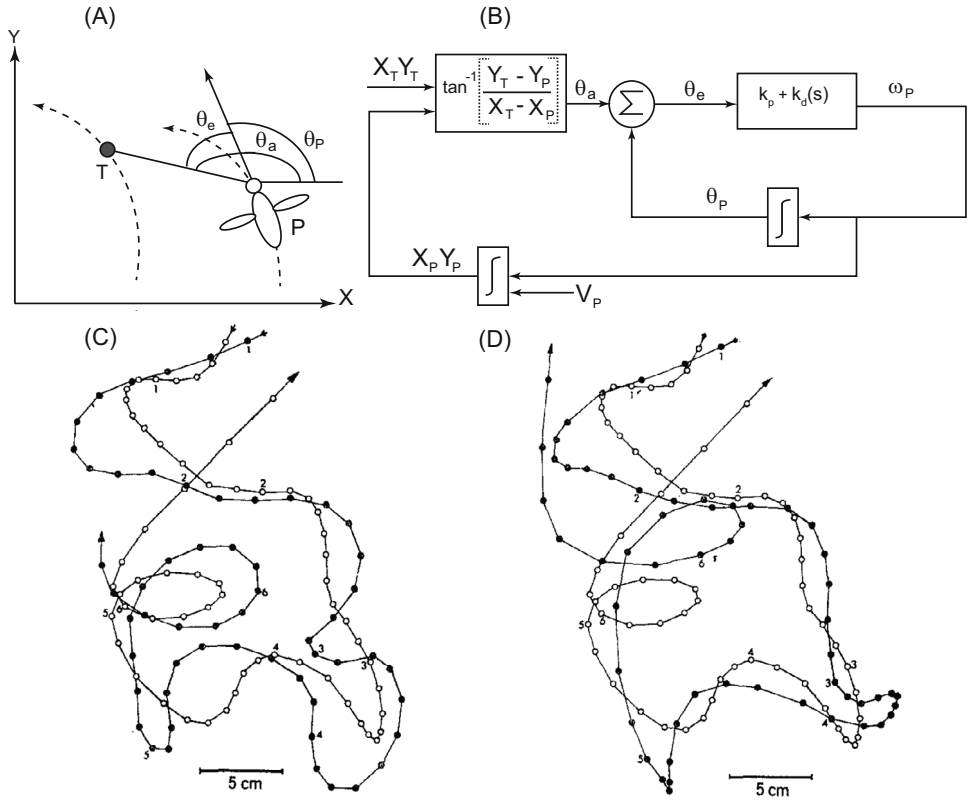

Fig. 1. (A) Geometry of smooth tracking between the target (T) and pursuer (P) houseflies, (B) illustration of the PD feedback control system used by the houseflies, (C) simulated chase sequence between conspecifics using a gain of $20\,\mathrm{s}^{-1}$ and delay of 30 ms where the hollow circles indicate the leading fly and filled circles indicate the chasing fly, (D) the actual chase sequence as observed experimentally (figures adapted and modified from [7]).

a simple illustration of the PD feedback control system used by *Fannia canicularis*. The angle θ_a can be calculated from the pursuer co-ordinates $(X_P, Y_P$, in Fig. 1B) and the target co-ordinates $(X_T, Y_T$, in Fig. 1B). The variable V_p in Fig. 1B denotes the linear velocity of the pursuer. In regions close to the pursuer fly's long axis (where θ_e was close to 35°), the angular velocity of the pursuer, ω_p, was further controlled by a second variable, $\dot{\theta}_e$, the error angular velocity or the relative velocity between the pursuer and the target as shown in Fig. 1B. The constants k_p and k_d in Fig. 1B denote the proportional and derivative gains of the fly's PD control system.

Using experimental data, the authors demonstrated a linear correlation between the pursuer fly's angular velocity and the error angle and the error angular velocity between the pursuer and the prey at certain time delays in accordance to Eq. (1).

$$\omega_{p(t+d)} = k_p \theta_{e(t)} + k_d \dot{\theta}_{e(t)}. \tag{1}$$

The gains k_p and k_d of the fly's feedback system were determined as $20\,\mathrm{s}^{-1}$ and 0.7, respectively. The delay d was the response time of the fly's sensorimotor system and accounted for delays due to neural processing and motor actions and was about 30 ms for *Fannia canicularis*. The authors experimentally validated the correlation in Eq. (1) for error angles in the range of $35° > \theta_e > -35°$. For error angles beyond this

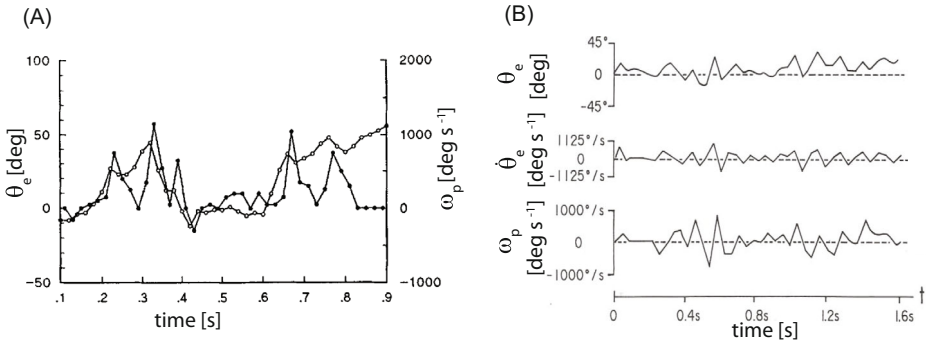

Fig. 2. (A) Time course of the error angle (θ_e) and pursuer angular velocity (ω_p) in dolichopidid fly pursuit sequences (adapted from [9]), (B) time course of error angle (θ_e), error angular velocity ($\dot{\theta}_e$) and pursuer angular velocity (ω_p) in the horizontal plane as observed in honeybees while tracking moving targets (adapted from [10]).

range, the authors experimental results didnot corroborate the proposed PD control mechanism. Using Eq. (1), the authors simulated flight paths and predicted the maneuvers of a pursuing fly for a known prey flight trajectory. The simulated trajectory as shown in Fig. 1C was in fair agreement with the actual trajectory (Fig. 1D) except in sharp bends and loops where the turns were broader while preserving most features of the actual chase sequence. The stable feedback gain for the fly's sensorimotor system predicted from simulations was $12.3\,s^{-1}$ for a delay of 30 ms, and was slightly higher than the experimentally obtained stable gain of $20\,s^{-1}$. In biological feedback systems with delays, oscillatory and unstable responses have been observed when the product of gain k and delay d exceeds $0.37(\frac{1}{e})$ [11]. For *Fannia*, the product (kd) was 0.6 indicating that the fly's feedback system was in between the limits of complete stability and instability [12].

A feedback system similar to *Fannia* was observed in male chase sequences of the dolichopodid fly *Poecilobothrus nobilitatus* [9]. However, unlike *Fannia*, *Poecilobothrus* used a simple proportional control, where the pursuer angular velocity ω_p was controlled only by the error angle θ_e input. Figure 2A shows the time course of the error angle θ_e and the angular velocity ω_p indicating a linear correlation. The system gain k was $30\,s^{-1}$ and the delay d in the fly's system was 15 ms. The product (kd) was 0.45 which indicated marginal stability in the fly's sytem. Zhang and coworkers showed that honeybees used a PD control system identical to *Fannia* in horizontal and vertical planes while tracking moving targets [10]. The tracking control positioned the honeybees to always locate their targets 35° below the bee's long axis. Figure 2B shows the temporal features of θ_e, $\dot{\theta}_e$ and ω_p while target tracking in the horizontal plane. The delay d in the bee's response time was approximately 40 ms. The authors investigated the chromatic properties of the tracking control and inferred that translational tracking was controlled by green-senstive receptors, whereas, the position error (θ_e) information involved signals from both green and blue sensitive receptors. In a relatively recent study with dummy targets, Boeddeker and coworkers revealed that male blowfly *Lucilia* employed smooth tracking in their pursuit and capture sequences [8,13]. The blowflies controlled the error angles in their frontal field to the target continuously as in Eq. (1) predominantly by smooth yaw rotations. In addition to error angle, the target size in the retina of the pursuer was also a decisive input variable which controlled the fly's forward speed. For the later case, the delay d in the fly's tracking control was about 60-80 ms. However, the system gain k and delay d values for the former were not resolved by the authors.

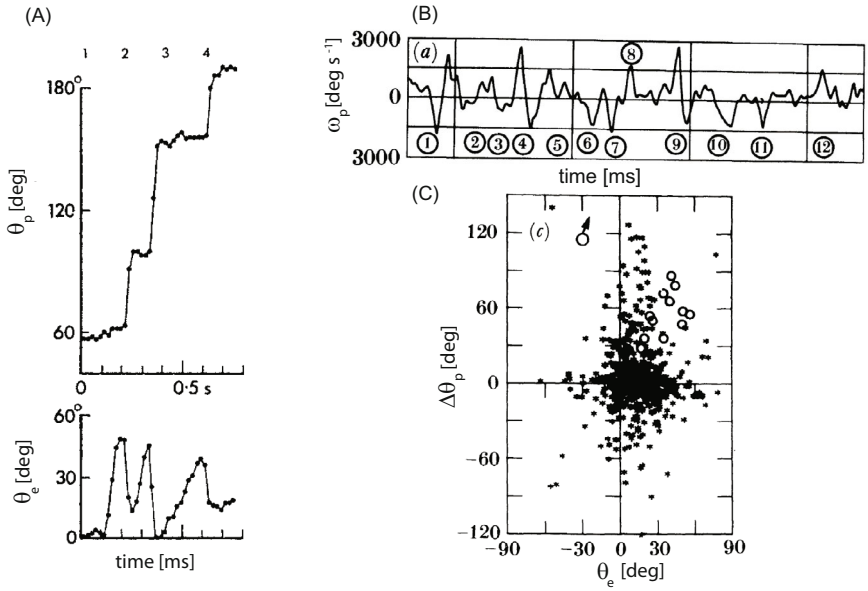

Fig. 3. (A) Angular position of the pursuing fly (θ_p) and error angle (θ_e) every 20 ms during saccadic tracking in *Syritta* (adapted from [14]), (B) time course of pursuer angular velocity about the transverse axis (ω_p) in *Musca* (adapted from [18]), (C) distribution of the saccadic amplitude ($\Delta\theta_p$) about the transverse axis with respect to the vertical error angle for *Musca* (the hollow circles mark turns right after take-off where translational movement is not dominant, adapted from [18]).

2.2 Saccadic tracking

Saccadic tracking or discontinuous tracking as referred by some researchers is a tracking phenomenon where the pursuer tracks a prey through a series of brief and rapid rotations of its entire body in synchrony with higher angular speed of the head and hence resulting in altered visual gaze and flight direction. The term "saccadic tracking" was coined by Collet and Land as it was analogous to human saccadic vision involving step-like rotational movements of the eye used to center stimuli and redirect gaze while shifting focus through a variety of tasks [14,15]. The saccadic tracking form has been shown to co-exist with smooth tracking in hoverflies, houseflies and blowflies [14,16,17].

Collet and Land discerned the coexistence of saccadic tracking with smooth tracking in pursuit studies with male hoverflies *Syritta pipiens* [14]. The switching between these tracking modes was strongly dependent on the location of the target image in the retina of the pursuer fly. The authors demonstrated that hoverflies conformed to the saccadic mode during very fast movements of the target or on sudden detection of a target which resulted the target image to shift to the peripheral retina of the pursuer. During these instances, the error angle (θ_e) between the pursuer and the target was greater than 8° before being corrected by the pursuing fly by employing a series of body rotations which reduced the θ_e. Figure 3A shows the temporal features of the angular position (θ_p) of the pursuer and the error angle (θ_e) during saccadic tracking. A series of saccades as evident in the pursuer angular position was made to reduce the error angle, the amplitudes of which ($\Delta\theta_p$) were correlated with θ_e. As evident in the figure, the saccadic turns made by the pursuer fly were not continuously controlled by θ_e, and thus the authors inferred that the saccadic tracking mode was

an open-loop and pre-programmed response of hoverflies to fast moving targets that didnot require a continuous visual input for feedback.

Wagner reported similar saccadic tracking strategies in the target pursuit of free-flying houseflies *Musca domestica* from detailed 3D analysis of pursuit trajectories [17–19]. The authors showed that the time profiles of angular velocities of the chasing houseflies about the vertical axis (yaw) and transverse axis (pitch) were characterized by a cascade of peaks which could be attributed to single body rotations of the fly with intermittent time periods of no rotations. Figure 3B depicts the time course of the pursuer angular velocity about the transverse axis (ω_p). Each saccadic turn or body rotation lasted for 10–30 ms and ranged upto 90° with strong correlations between the turning amplitudes ($\Delta\theta_p$) and the error angle θ_e. Figure 3C shows the linear correlation for a male fly with a cross correlation coefficient (r) of 0.4 between the two variables. The quantitative characteristics of the saccadic tracking mode were not presented by the authors.

It is evident from the saccadic tracking mechanism, that the turns or body rotations of the pursuer were based on a single input variable, the initial position error or θ_e of the pursuer with respect to the target, thus indicating open-loop control. Experimental results from houseflies and hoverflies suggest that the saccadic tracking mode complemented smooth or continuous tracking mode during those phases of target pursuit where the target θ_e was fairly large. For such phases, which would mostly occur during very fast target movements, after sensing the initial θ_e, the pursuing fly would undergo several body rotations or saccades to compensate for the rapidly changing θ_e. A possible reason for such behavior as pointed out by Land and Collet was the differential resolving power of the fly's eye, where the forward directed region or the fovea had a higher resolution as compared to regions outside the fovea. Consequently, when targets were located outside the fovea, the flies used saccadic control, whereas targets fixated within the fovea were tracked by smooth tracking mechanism [14].

2.3 Interception

Some aerial species use interception as a mechanism to pursue and capture their targets. During the interception mode, the pursuer instead of continuous tracking, aims at a point in front of the projected flight path of the target. The resulting pursuer trajectory is a straight line that intersects with the target flight path. Interception was observed as a pursuit strategy in male hoverflies of the genus *Eristalis* and *Volucella* by Collet and Land [20].

Collet and Land discerned the interception mode of tracking targets in male hoverflies in their responses to approaching projectiles launched to them. The interception course adopted by the pursuer was based on two known variables detected by the stationary pursuer; the target angular position (θ_T) at first sighting with respect to the pursuer body axis, and the target angular velocity relative to the stationary pursuer ($\dot{\theta}_T$). Figure 4A shows the geometry of interception for the pursuer. According to the authors calculations, interception occured when the pursuer adopted a course with an interception angle β relative to the first line of sighting TP so that the paths PI and TI were covered in the same time t by the pursuer and the target, respectively. The inteception angle β was calculated from Eq. (2):

$$\beta = 180 - sin^{-1}\left(\frac{2v}{at} sin\alpha\right) \tag{2}$$

where v and a denoted the constant target velocity and the constant pursuer acceleration which were genetically known variables to the hoverfly since the interception

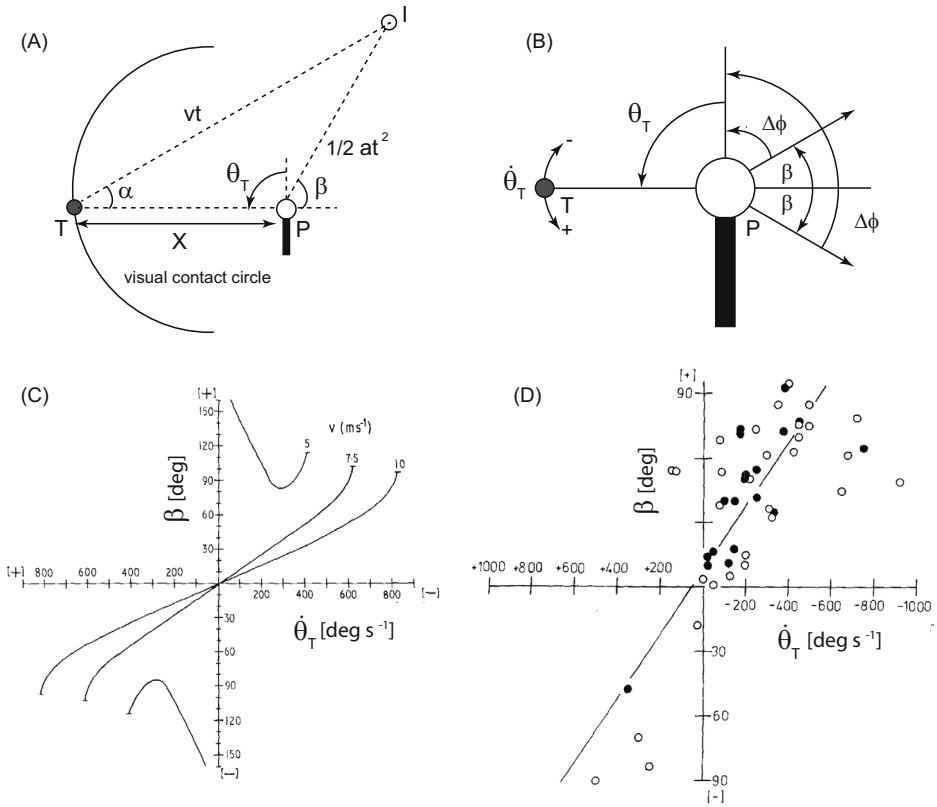

Fig. 4. (A) Geometry of the interception course for a pursuer hoverfly (P) to intercept its target (T) with an interception angle β relative to the first line of sighting TP, (B) size of the turn ($\Delta\phi$) required by the hoverfly for succesful capture, (C) predicted plots of interception angle as a function of target angular velocity at the time of first sighting for different target velocities (v), (D) actual correlation between the above variables in male hoverflies chasing dummy targets where filled circles indicate data from *Eristalis* and hollow circles indicate data from *Volucella* (figures adapted and modified from [20]).

strategy was adopted by the males in catching their female counterparts only. Male hoverflies have been reported to have an acceleration capability of 30 to 35 ms^{-2} and maximum velocity in the range of 7.5 to 10 ms^{-1} by the authors [20]. The angle α denoted the approach angle of the pursuer fly which could be estimated from the target angular velocity relative to the stationary pursuer $\dot{\theta}_T$, and the variable x, the distance at which the target became visible, which was also a genetically known variable to the pursuer according to Eq. (3).

$$\alpha = sin^{-1}\left(\dot{\theta}_T.\frac{x}{v}\right). \tag{3}$$

The authors deduced a simple rule as expressed in Eq. (4) for the size of the turn $\Delta\phi$ (shown in Fig. 4B) that a male hoverfly should make during its initial turns for succesful capture of their female counterparts from their experimental observations.

$$\Delta\phi = \theta_T - 0.1\dot{\theta}_T \pm 180^\circ. \tag{4}$$

For example, if the pursuer located a target at 90° in the counterclockwise direction and if the target angular velocity ($\dot{\theta}_T$) at that instant was 500°s^{-1} clockwise, then the

accurate size of the turn for the interception course would be 40° counterclockwise as calculated from Eq. (4). To validate the above model, the authors compared the predicted values of the interception angle (β) with experimental data from *Eristalis* and *Volucella*. Figure 4C shows the plot of β as a function of relative angular velocity $\dot{\theta}_T$ as predicted from Eq. (2) and Eq. (3) for different target velocities, and, Fig. 4D shows the actual correlation between the above variables. When the acceleration, target speed and the sighting distance values were $35\,\mathrm{ms}^{-2}$, $7.5\,\mathrm{ms}^{-1}$ and $0.7\,\mathrm{m}$, respectively, then the predicted correlation between β and $\dot{\theta}_T$ was $\beta = 0.1\dot{\theta}_T$ whereas the experimental correlation from data was $\beta = 0.13\dot{\theta}_T$ which was statistically significant(P<0.001).

Hence, it can be inferred that target capture using the interception mode is an example of an open loop control similar to saccadic tracking as the pursuer's initial turns were based on single inputs of the target position and relative angular velocity at first sighting in contrary to smooth tracking which is an example of a closed-loop response.

2.4 Motion camouflage

Motion camouflage is a deceptive mode of tracking where the pursuer poses as an immobile object in the retina of the moving target while tracking and approaching it. As a pursuer such as an insect moves, the images of the surrounding objects in the environment move simultaneously in its retina even though the objects are stationary, thus, producing an optic array of time frozen images called optic flow [21]. In the self-moving state, the optic flow produced from stationary and moving objects in the insect retina are inconsistent which facilitates distinction between them [22]. However, some predatory insects such as hoverflies of the species *Syritta pipiens* and dragonflies of the species *Hemianax papuensis* have developed deceptive mechanisms as motion camouflage to eliminate discrepancies in the optic flow field from stationary and mobile objects while tracking their conspecifics [23,24]. Srinivasan and Davey proposed a simple approach for motion camouflage which involved self adjustment of a predator's motion in a manner that mimicked the image motion of a stationary object in the prey retina [23]. For example, if a predator (P) wished to shadow a target (T) and imitate itself as a fixed object at the camouflage point (C), this could be achieved if the predator always moved in a straight line connecting the points (T) and (C) called the "camouflage constraint line". A number of trajectories would be possible for the predator. Figure 5A and Fig. 5B show the resulting trajectories when the pursuer appear as stationary points behind itself and at infinite distance away from itself, respectively. The authors proposed that the predator could remain in the camouflage constraint line following a set of simple guidelines: viewing the prey frontally, and pointing radially away from the camouflage point. To accomplish this, the predator needed to make simple corrective yaw rotations $\Delta\theta$ and corrective lateral motions $\Delta\lambda$, to adjust its current distance ρ from the camouflage point C (illustrated in Fig. 5C) according to Eq. (5).

$$\rho = \frac{\Delta\lambda}{\Delta\theta}. \tag{5}$$

Equation (5) could be derived from the basic definition of radians since the lateral displacement and the radial distance of the pursuer from the camouflage point C are coupled through the yaw angular rotation for small angular rotations. Thus, knowledge of any one of the variables is sufficient for self adjustment of the pursuer's motion. The authors argued by refering to several biological species that the pursuer could be aware of its current distance ρ from the camouflage point and hence would adjust the

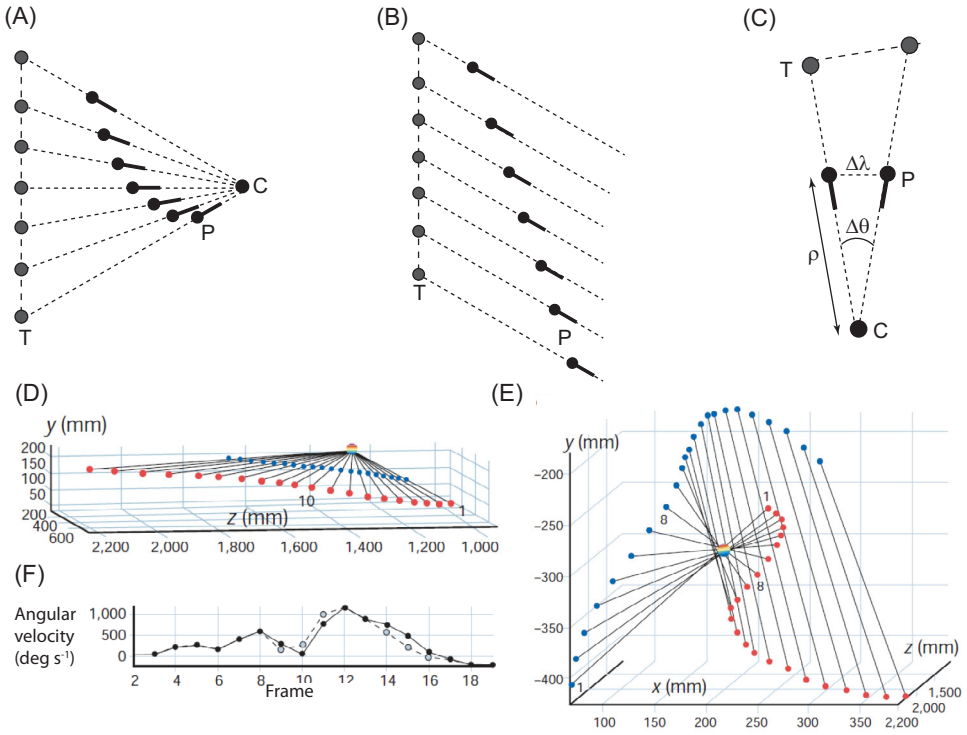

Fig. 5. Illustration of motion camouflage strategies where the pursuer (P) poses as a virtual stationary object to the target (T) at (A) a camouflage point behind itself, and (B) infinite distance away from itself, (C) illustration of the required correlation between corrective yaw rotation ($\Delta\theta$) and corrective lateral motion ($\Delta\lambda$) of the pursuer for motion camouflage, Active motion camouflage data acquired between head positions of two dragonflies at 20 ms steps where the shadower poses as a stationary object (D) behind itself and (E) in front of itself and at infinite distance away, (F) comparison of the angular velocity profiles produced by the shadower dragonfly and a virtual stationary object in the shadowee's eye (figures adapted and modified from [23] and [24]).

coupling coefficent between the lateral motion and yaw rotation to adjust ρ. Equation (5) is valid for any radial distance and any radial speed chosen by the pursuer. However, if the pursuer's speed is specified to a fixed value, then the trajectory of the pursuer would be determined by the shadowee's or target's motion and the pursuer's only freedom would be in determining whether to approach or retreat from the target.

Most of the experimental work on the motion camouflage concept have been performed by Srinivasan and coworkers. In male hoverflies *Syritta*, the authors re-examined previously published flight trajectories of conspecifics from Land and Collet and validated that they emulated as a quasi-stationary object [23]. In a separate study, the authors demonstrated active motion camouflage between two male dragonflies *Hemianax* by reconstructing three dimensional flight trajectories of their territorial maneuvers [24]. They revealed that the pursuer males shadowed their female counterparts by emulating as stationary objects in front of themselves (Fig. 5D) or at infinite distance away from their targets (Fig. 5E). The intersection spheres of their camouflage constraint lines were approximately in between 8.5 mm and 11.3 mm in radius. The authors also compared the angular velocity profiles of the

pursuer dragonfly and a virtual stationary object at the camouflage point as shown in Fig. 5F. Both profiles matched closely thus affirming motion camouflage as a possible stealth strategy in these species.

Justh and Krishnaprasad suggested a steering control law that could lead to motion camouflage while being biologically feasible [25]. The authors modeled the pursuer and the prey as a system of point particles and derived the following motion camouflage control law with respect to a point at infinity. The control law was dependant on the transverse component of the relative velocity between the pursuer and the prey as shown in Eq. (6).

$$u_p = -\mu \left(\frac{r}{|r|} . \dot{r}^{\perp} \right) \tag{6}$$

where u_p was the steering control input of the pursuer, μ was the control gain and r was the relative vector from the pursuer to the prey. The critical sensor measurement necessary for the pursuer to achieve motion camouflage adopting the above control law was the angular speed of the target across its retina which could yield information on the transverse relative velocity.

2.5 Constant absolute target direction

In the constant absolute angle target direction (CATD) mechanism, the position vector from the pursuer and the target is at a fixed angle with the horizontal throughout the pursuit scenario. This fixed angle is referred to as the absolute angle. The CATD mode of tracking and interception is a subset of the motion camouflge concept where the pursuer shadows a prey from an infinite distance away. Literature reveals that hoverflies and big brown ecolocating bats adopt this strategy while capturing their quarry [26,27].

Olberg and coworkers analyzed the prey pursuit of male dragonflies *Erythemis simplicicollis* and *Leucorrhinia intacta* [26]. Measurements of error angle (θ_e) and absolute angle (θ_a) of the above species to their prey revealed an average variation of 2.8° in θ_a as opposed to a variation of 8.0° in θ_e. Figure 6A shows the absolute angle and error angle variations in *Leucorrhinia* as recorded by the authors. Due to smaller variations in θ_a during a pursuit sequence, the authors inferred that dragonflies steered to maintain their absolute angle constant.

In a fairly recent experimental study with echolocating big brown bats *Eptesicus fuscus*, Moss and coworkers demonstrated the use of the constant absolute angle mechanism in pursuit and interception of erratically moving targets [27]. From 3D analysis of bat trajectories, the authors revealed that big brown bats steered to minimize the deviation of their absolute angles to the target while keeping head locked on to the target. Figure 6B illustrates the CATD strategy where θ_a denotes the absolute angle and θ_e denotes the error angle also referred to as bearing angle by the authors. The authors introduced an error term ϕ_e that defined the deviation of the actual error angle or bearing angle from the optimum error angle $\theta_{e(opt)}$ (the error angle that leads to interception in minimum time) as in Eq. (7).

$$\phi_e(t) = \theta(t) - \theta_{e(opt)}(t). \tag{7}$$

The authors argued that if the bats maneuvered to use the CATD mechanism, then the rate of change of θ_a would be zero (i.e. $\dot{\theta}_a \rightarrow 0$). On the contrary, if it only maintained a constant bearing, then the rate of change of θ_e would be zero (i.e. $\dot{\theta}_e \rightarrow 0$). Figure 6C shows the trajectories of the pursuer and the prey and Fig. 6D

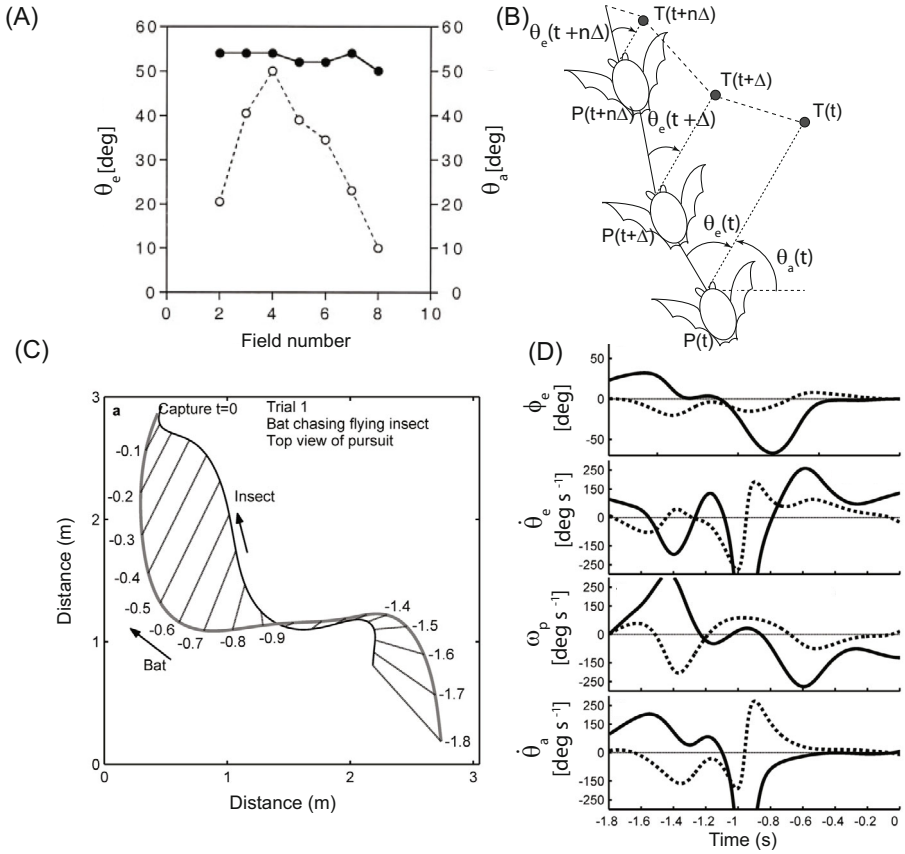

Fig. 6. (A) Variation of absolute angle (filled circle) and error angle (hollow circle) in the dragonfly *Leucorrhinia* (from [26]), (B) the time-optimal constant absolute target direction strategy (CATD) in *Eptesicus* (from [27]), (C) the trajectories of *Eptesicus* and a flying insect during a chase sequence (from [27]) and (D) pursuit parameters during the chase sequence: error term (ϕ_e), rate of change of error or bearing angle ($\dot{\theta}_e$), pursuer angular velocity ω_p, and rate of change of absolute angle ($\dot{\theta}_a$) (from [27]).

shows data supporting the CATD strategy. As evident in Fig. 6D, the maneuvers of the bat were directed to driving $\dot{\theta}_a \to 0$, while $\dot{\theta}_e$ did not approach zero. The authors argued that by driving $\dot{\theta}_a \to 0$, the pursuer bat could maintain an optimum bearing $\theta_{e(opt)}$ to the target, such that at every instant, the error term ϕ_e would also approach zero ($\phi_e \to 0$).

The authors used a delay differential equation to model their ϕ_e data as shown in Eq. (8).

$$\dot{\phi}_{e(t)} = k\phi_e(t - \tau) \tag{8}$$

where k was the model gain and τ was the system delay. The values of the model gain and delay that best satisfied the model were $3.55\,\mathrm{s}^{-1}$ and 120 ms, respectively. The authors estimated that the system delay in the bat τ included components for echo travel time (τ_{echo}) which was ≤ 12 ms, for neural mechanisms involved in auditory processing ($\tau_{auditory}$) which was about 20 ms, and for motor processing τ_{motor} which accounted for the remaining time. However, in the pursuit of conspecifics and tethered targets, the big brown bats were shown to conform to a constant bearing mode of

tracking in which the bearing θ_e to the target was held fixed or approached zero (i.e. $\dot{\theta}_e \rightarrow 0$) during the interception phase as opposed to the CATD mode.

In a different experimental study, Moss and coworkers linked the sonar vocalizations of the echolocating bats to their flight directions through an adaptive linear law [28]. The authors computed the acoustic gaze direction or the direction of the sonar beam axis of the echolocating bats (θ_{gaze}) from reconstructed sonar beam patterns and showed its correlation with the bat's flight angular velocity ($\dot{\theta}_{flight}$) through the following control law Eq. (9).

$$\dot{\theta}_{flight(t+\tau)} = k\theta_{gaze} \tag{9}$$

where k was the state-dependent gain factor and τ was the lag time between the acoustic direction and the flight angular velocity. The state-dependent gain value k varied in the search and approach, tracking and attack phases of prey capture (three well known phases in prey pursuit of echolocating bats) between 3.21 and 6.26 s^{-1} and the maximum lag time (τ_{max}) between 148 and 96 ms.

3 Pursuit and optomotor response

Vision based pursuit sequences are complex as a pursuer's turn toward a target can cause it's retinal image to shift in the reverse direction. This may result in optomotor reflexes that can drive the pursuer away from its target thus impeding the pursuit sequence. Researchers have investigated the optomotor reflexes and their interaction with the target pursuit system through behavioural studies where the pursuit sequence is facilitated in an environment artificially perturbed or moved around the experimental setup. Such inteactions have been well characterized in target pursuit studies with hoverflies and blowflies [29,30].

Three schemes of interaction between target pursuit and optomotor response, namely additive, efference copy and suppressive, has been well documented in literature. In the additive scheme (Fig. 7A), the turning response or the resulting angular velocity of the pursuer (ω_p) is a summation of the response due to change in error angle (θ_e) which is the input to the pursuit system, and the response due to change in angular velocity of the background (ω_{bg}) which is the input to the optomotor system. The effect of the optomotor system is smaller when the gain of the pursuit system (g_p) is higher than the gain of the optomotor system (g_o). In the efference copy scheme (Fig. 7B), as the name indicates, a copy of the output from the pursuit system is added as an input to the optomotor system, and the turning response is still a summation of the responses form the individual systems. In the suppressive scheme (Fig. 7C), a copy of the output from the pursuit system reduces the optomotor gain and supresses the response of the optomotor system. In other words, in this scheme, the optomotor response remains inactive during the pursuit response.

The interaction between the optomotor response and the tracking response was investigated in the hoverfly *Syritta* through a rotating drum experiment where the drum velocity represented ω_{bg} and the retinal target position represented θ_e [29]. From experiments, the authors inferred that the flies turning response followed the additive or the efference scheme of interaction. The tracking gain g_p in such case was 30–40 s^{-1} and the optomotor gain g_o was 0.8. The tracking gain differed from the optomotor gain in a frequency dependent manner, where the pursuit system responded strongly at high frequencies for transient target movements whereas the optomotor system responded best at low frequencies. In male blowflies, the dynamics and performance of the pursuit sequence was not affected in the presence of a background moving in the same or opposite direction [30]. Thus the authors inferred that the blowflies

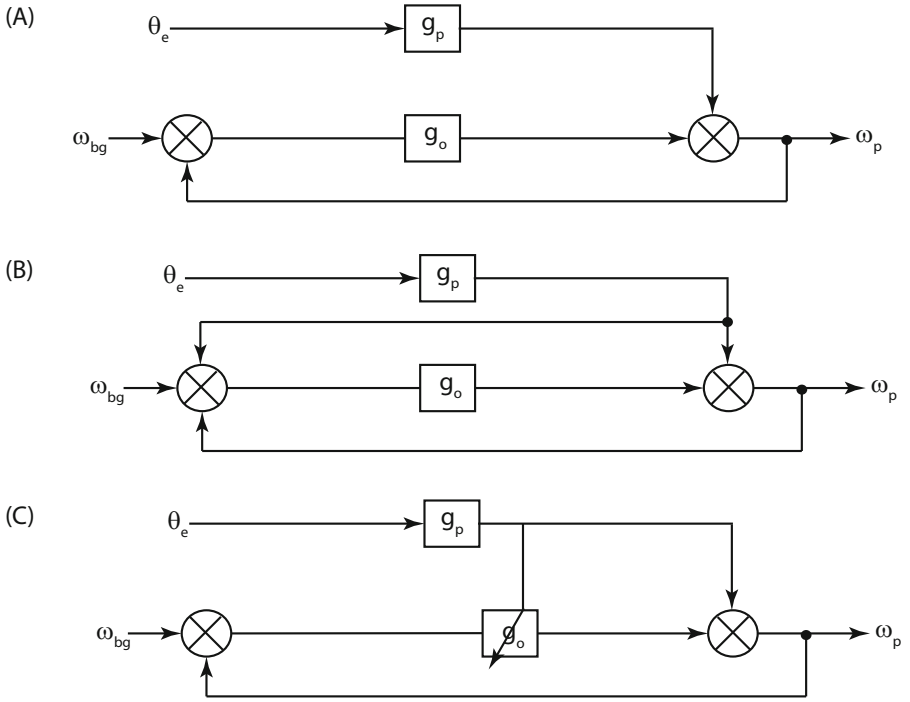

Fig. 7. Possible forms of interaction between the pursuit system and the optomotor system in aerial insects (A) Additive scheme (B) Efference copy scheme and (C) Suppressive scheme (adapted from [30]).

adhered to a suppressive scheme of target pursuit, where the optomotor system was largely suppressed by the chasing system.

4 Discussion and conclusion

The neural mechanisms underlying specific target pursuit maneuvers in aerial insects and bats have been investigated by several researchers. In most flies, visual flight control is triggered by the large-field motion-sensitive neurons that are located in the third neuropile layer, the lobula plate. The lobula plate tangential cells are preferentially sensitive to vertical (VS cells) and horizontal (HS cells) motion, respectively [31]. In honeybees, a group of 12 neurons in the ventral nerve cord called the velocity-tuned (VT) cells have been found to be sensitive to horizontal motion [32]. However, target detection and specificity during aerial target pursuit, have been linked to different sets of neurons in different aerial species. For example, in dragonflies, a group of specific neurons in the ventral nerve cord of the optic lobes called the target selective descending neurons (TSDNs) play a role in the directional responses of the fly to small target movements, responses to increased target angular speed, in steering movement of the wings of the fly and also in predicting future target location. These TSDNs are the largest and fastest axons in the nerve cords of the dragonfly [1,33]. The saccadic turns made by the housefly *Musca domestica* during target pursuit have been linked not only to the HS cells but also to gyroscopic organs called halters that are sensitive to high angular velocities of the targets [19]. Similarly in blowflies, a certain set of sex-specific neurons called Male Lobula Giant 1 (MLG1) in the third visual neurophil has been linked to target specificty during chase sequences. The MLG1 neurons in

blowflies show distinct directional specificity and nonlinear response characteristics to different parameters such as size, position and velocity and to variations in these parameters [34]. In a different study, authors have shown that the lobula plate tangential cell H1 or the H1 neuron in the blowfly *Lucila* is tuned to detect higher velocities during locomotion [35]. Clandinin and deVries have shown that the Foma-1 neurons in the fruitfly *Drosophila* are targeted to detect looming objects while on a collision course with a fly [36].

In insectivorous bats, the repetition rate of the echolocation calls rapidly vary while approaching the prey and are characterized into phases of search, approach and terminal [37]. Certain "delay-tuned" neurons in the mid-brain of the echolocating bats have been found to be sensitive to temporal delays in the sonar cry and echo and encode information on target distance and dimension that are linked to prey pursuit behavior [38,39].

It is evident from the different pursuit approaches investigated todate that the target angular position with respect to the pursuer plays a key role in the prey capture dynamics. The angular position information is perceived in different forms such as error angle, absolute angle or bearing angle by each pursuing species for target capture. The actions of the pursuer (e.g. the change in the angular velocity) are guided by an open loop or closed loop sensorimotor control system. Although the underlying neural mechanism behind target detection and pursuit has been intensely investigated for some aerial species in recent years, however, further research is necessary to close the loop between these different behavioral strategies and sensorimotor responses. The same applies to the studies on prey capture dynamics in different aerial species. Most behavioral experimental studies have deduced capture strategies assuming the pursuer and target as point particles. However, examining flight capture dynamics using rigid body models of the pursuer and the prey, including aerodynamic effects while analyzing the capture dynamics, and linking the prey capture mechanism to the neural models of sensory input would provide a comprehensive knowledge of the underlying control mechanisms employed by the prey in capture of its quarry. This can expand the current applications of these strategies in navigation and control of engineered systems.

Some current areas of application of prey capture strategies include missile guidance systems; design and control of autonomous aerial vehicles such as unmanned aerial vehicles (UAVs) and micro-UAVs for search and rescue missions, for security work and for spy and attack missions; in co-operative control of multi-agent systems; in radar jamming and deception and in designing robotic models. Of the different prey capture mechanisms, the motion camouflage approach has received the most attention to date in terms of application. The cohesive properties of the motion camouflage approach has been applied by researchers in autonomous vehicle control, phantom track generation and co-operative control [40–42]. As example, Yonghong and coworkers have demonstrated that a bio-inspired guidance law based on motion camouflage has improved ballistics and flight performance for small aerial vehicles during the terminal guidance phase as opposed to when a proportional guidance law is applied [43].

The author is sincerely thankful to the late Prof. Suhada Jayasuriya for his guidance and support in the initial phases of the manuscript. The author would also like to thank the National Science Foundation for financial support under grant number CMMI-1134669.

References

1. R.M. Olberg, A.H. Worthington, K.R. Venator, J. Comp. Physiol. A **19**, 155 (2000)
2. A. Borst, Curr. Biol. CB **19**, R36 (2009)

3. R.M. Olberg, Curr. Opin. Neurobiol. **22**, 267 (2012)
4. M.V. Srinivasan, Curr. Opin. Neurobiol. **21**, 535 (2011)
5. A.J. Simmons, M.B. Fenton, M.J. O'Farrell, Science **203**, 16 (1979)
6. C.F. Moss, A. Surlykke, J. Acoust. Soc. Am **110**, 2207 (2001)
7. M.F. Land, T.S. Collet, J. Comp. Physio. **89**, 331 (1974)
8. N. Boeddeker, R. Kern, M. Egelhaaf, Proc. Biol. Sci. **270**, 393 (2003)
9. M.F. Land, J. Comp. Physiol. **173**, 605 (1993)
10. S.W. Zhang, X.A. Wang, Z.L. Liu, M.V. Srinivasan, Vis. Neurosci. **4**, 379 (1990)
11. B. Hassenstein, *Information and control in the living organism: an elementary introduction* (Chapman and Hall, London, 1971), p. 100
12. M.F. Land, J. Insect Physiol. **38**, 939 (1992)
13. N. Boeddeker, M. Egelhaaf, Proc. Biol. Sci. **270**, 1971 (2003)
14. T.S. Collet, M.F. Land, J. Comp. Physiol. **99**, 1 (1975)
15. M.F. Land, M. Hayhoe, Vision Res. **41**, 3559 (2001)
16. N. Boeddeker, M. Egelhaaf, Proc. Biol. Sci. **208**, 1563 (2005)
17. H. Wagner, Philos. Trans. R. Soc. B Biol. Sci. **312**, 527 (1986a)
18. H. Wagner, Philos. Trans. R. Soc. B Biol. Sci. **312**, 553 (1986b)
19. H. Wagner, Philos. Trans. R. Soc. B Biol. Sci. **312**, 581 (1986c)
20. T.S. Collet, M. F. Land, J. Comp. Physiol. **125**, 191 (1978)
21. D.N. Lee, Philos. Trans. R. Soc. Lond. B. Biol. Sci. **290**, 169 (1980)
22. M. Leherer, M.V. Srinivasan, J. Comp. Physiol. **171**, 457 (1992)
23. A. Mizutani, J.S. Chahl, M.V. Srinivasan, Nature **423**, 604 (2003)
24. M. Davey, M.V. Srinivasan, Proc. R. Soc. Lond. B Biol Sci. **259**, 19 (1995)
25. E.W. Justh, P.S. Krishnaprasad, Proc. R. Soc. A **462**, 3629 (2006)
26. R.M. Olberg, A.H. Worthington, K.R. Venator, J. Comp. Physiol. A **186**, 155 (2000)
27. K. Ghose, T.K. Horiuchi, P.S. Krishnaprasad, C.F. Moss, PLoS Biol **4**, 10 (2006)
28. K. Ghose, C.F. Moss, J. Neurosci. **26**, 1704 (2006)
29. T.S. Collet, J. Comp. Physiol. **140**, 145 (1980)
30. C. Trischler, R. Kern, M. Egelhaaf, Front. Behav. Neurosci. **4**, 1 (2010)
31. A. Borst, J. Haag, D.F. Reiff, Ann. Rev. Neurosci. **33**, 49 (2010)
32. M.R. Ibbotson, Proc. R. Soc. Lond. B **268**, 2195 (2001)
33. T.L. Adelman, W. Bialek, R.M. Olberg, Neuron **40**, 823 (2003)
34. C. Trischler, N. Boeddeker, M. Egelhaaf, J Comp Physiol A **193**, 559 (2007)
35. S.N. Jung, A. Borst, J. Haag, J Neurosci. **31**, 9231 (2011)
36. S.E.J. de Vries, T.R. Clandinin, Curr. Biol. **22**, 353 (2012)
37. D.R. Griffin, F.A. Webster, C.R. Michael, Anim. Behav. **8**, 141 (1960)
38. A.S. Feng, J.A. Simmons, S.A. Kick, Science **202**, 645 (1978)
39. S.P. Dear, N. Suga, J. Neurophysiol. **73**, 1084 (1995)
40. A.J. Anderson, P.W. McOwan, Proc. International. Joint Conference. on Neural Networks **3**, 2006 (2002)
41. Y. Xu, G. Basset, American Control Conf. **73**, 5400 (2010)
42. D.J. Kwak, B. Choi, H.J. Kim, Intell. Rob. Appl. **72**, 594 (2013)
43. W. Zhengjie, H. Weilin, Y. Yonghong, Chin. J. Aeronautics **28**, 260 (2015)